富山大学研究推進機構水素同位体科学研究センター研究報告 39：1－8，2019.

論　文

窒素プラズマ処理した$LaTa_2O_7$ナノシート光触媒による トリエタノールアミン水溶液からの水素生成反応

萩原　英久、早川　克明、野澤　一徳

富山大学 研究推進機構 水素同位体科学研究センター
〒930-8555　富山市五福 3190

Photocatalytic hydrogen production from triethanolamine aqueous solution by $LaTa_2O_7$ nanosheets treated with nitrogen plasma

Hidehisa Hagiwara, Katsuaki Hayakawa, Ittoku Nozawa

Hydrogen Isotope Research Center, Organization for Promotion of Research,
University of Toyama, Gofuku 3190, Toyama, 930-8555, Japan

(Received March 31, 2020; accepted August 7, 2020)

Abstract

N-doped $LaTa_2O_7$ nanosheets (LTON-BP) were prepared by polygonal barrel-plasma surface modification method using N_2 plasma. X-ray photoelectron spectroscopy measurements suggest that nitrogen atoms were added at the interstitial crystal lattice sites of the N_2 plasma-treated photocatalyst. The photocatalytic activity of LTON-BP for H_2 production from triethanolamine aqueous solution was found to be 3.3 times higher than that of N-doped $LaTa_2O_7$ nanosheets prepared by a conventional method, which is attributed to the high oxidation ability of LTON-BP stemming from its band structure.

1. Introduction

Photocatalytic water splitting is a promising process for hydrogen production because hydrogen can be generated from sunlight and water without emission of carbon dioxide. Since the report by Jansen and Letschert in 2000 on the photocatalytic activity of a mixed anion compound [1], oxynitrides have been actively studied as visible light-responsive

photocatalysts [2-6]. It has been reported that the solid solution of $LaTaON_2$ and $LaMg_{1/3}Ta_{2/3}O_3$ is suitable for water splitting under visible light with a wavelength shorter than 600 nm [7]. However, the resulting solar-to-hydrogen conversion efficiency is as low as 0.2% [8], and further research is required. Meanwhile, metal oxide nanosheets prepared from the exfoliation of layered metal oxide have recently emerged as promising photocatalyst materials. Oxide nanosheets are two-dimensional anisotropic semiconductors having several nanometers of thickness and several micrometers of lateral dimension, and are characterized by high crystallinity and large surface area. These features provide advantages such as suppression of recombination of photoexcited charges and reaction site separation, which renders the oxide nanosheets suitable for photocatalysis. This has prompted the interest in nitrogen-doped oxide nanosheets, and several studies on their synthesis have been reported [9,10]. In the conventional preparation method of N-doped oxide nanosheets, a layered metal oxide is heated under NH_3 gas flow at high temperature (>1073 K), and is then exfoliated by acid treatment and amine intercalation. This conventional process has some drawbacks, particularly regarding the generation of impurities such as metal nitrides and coarsening of particles by high-temperature heat treatment, which hinders the exfoliation step. To avoid these problems, we employ in this study a polygonal barrel-sputtering method using N_2 plasma to synthesize N-doped oxide nanosheets by direct nitridation of $LaTa_2O_7$ nanosheets. The photocatalytic activity of the as-prepared N-doped $LaTa_2O_7$ nanosheets is evaluated and compared with that of N-doped $LaTa_2O_7$ prepared by a conventional NH_3 heating process.

2. Experimental

2.1. Photocatalyst preparation and characterization

All reagents were used without further purification. The layered oxide $RbLaTa_2O_7$ was synthesized by heating a mixture of Rb_2CO_3 (97.0%, Wako Pure Chemical Industries, Ltd., Japan), La_2O_3 (98.0%, Wako Pure Chemical Industries, Ltd., Japan), and Ta_2O_5 (99.9%, Kojundo Chemical Lab. Co., Ltd., Japan) at 1373 K for 12 h in air. The molar ratio of the mixture was Rb:La:Ta = 1.5:1:2. An excess amount (50 mol%) of $RbCO_3$ was added to compensate for volatilization loss. The as-synthesized $RbLaTa_2O_7$ (2.0 g) was added to an Erlenmeyer flask (300 mL) along with 1 M HCl (150 mL), and the mixture was shaken for a week to exchange rubidium to proton. The protonated sample was collected by centrifugation and dried in vacuum. The obtained $HLaTa_2O_7$ (1.0 g) was stirred in 1 M ethylamine (EA)

aqueous solution (100 mL) for three days to intercalate the EA into the interlayer. The EA-treated sample (0.5 g) was stirred for three days in 100 mL of a 0.025 M tetrabutylammonium hydroxide (TBAOH) aqueous solution to exfoliate into $LaTa_2O_7$ nanosheets (LTO). The N-doped $LaTa_2O_7$ nanosheets (LTON-BP) were synthesized from LTO using a polygonal barrel-plasma surface modification method (RF output: 200 W, N_2 pressure: 7 Pa, time: 1 h) as reported elsewhere [11]. For comparison, a different sample of N-doped $LaTa_2O_7$ nanosheets (LTON-NH) was prepared by heating $RbLaTa_2O_7$ at 1073 K under NH_3 flow (200 mL/min) for 5 h, followed by exfoliation as described above.

X-ray diffraction (XRD) patterns of the samples were obtained with an X-ray diffractometer (D8 DISCOVER, Bruker AXS) equipped with Cu Kα radiation (tube voltage: 45 V, current: 40 mA). Surface morphology observation and composition analysis were performed with a scanning electron microscope equipped with an energy dispersive X-ray spectrometer (SEM-EDX: JSM-6701F, JEOL). X-ray photoelectron spectroscopy (XPS) was conducted using an X-ray photoelectron analyzer (ESCALAB 250Xi, Thermo Fisher Scientific). Ultraviolet–visible (UV–vis) diffuse reflectance spectra were measured using a UV–vis spectrophotometer (V-560, JASCO Corporation) equipped with an integrating sphere unit. The optical band gap was determined using Tauc's equation (1) [12]

$$(\alpha h\nu)1/n = A(h\nu - Eg), \quad (1)$$

where A is a constant, hν is the photon energy, Eg is the energy gap, n = 1/2 for allowed direct transition, and n = 2 for allowed indirect transition. Since the $RbLaTa_2O_7$ compounds used in this study are indirect transition semiconductors [10], n = 2 was used to prepare the Tauc plot.

2.2. Photocatalytic reaction

To evaluate the photocatalytic activity, a closed-circulation reactor with a quartz reaction cell was used. The photocatalyst powder (10 mg) and $Pt(NH_3)_4(NO_3)_2$, which was used as Pt cocatalyst precursor for H_2 production, were added to 0.75 M of a triethanolamine (TEOA) aqueous solution (25 mL) in the quartz reaction cell. Then, the reaction cell was irradiated with an Xe lamp (2.0 W/cm) under magnetic stirring. The evolved gases were detected using a gas chromatograph (GC-8A, Shimadzu Corp., Japan) with a thermal conductivity detector.

3. Results and Discussion

Figure 1 shows the XRD pattern of the prepared $LaTa_2O_7$ nanosheets (LTO), which is in accordance with that previously reported [10]. The sheet-like structure of LTO, which is composed of La and TaO_6 octahedral units, is shown in Figure 2. Figure 1 also displays the diffraction pattern of LTON-NH obtained by exfoliation of heat-treated $RbLaTa_2O_7$ in NH_3 atmosphere, and that of LTON-BP, which was prepared by N_2 plasma treatment using a polygonal barrel-sputtering method. Since the diffraction patterns of LTON-NH and LTON-BP were similar to that of LTO, it can be assumed that all samples have similar crystal structures.

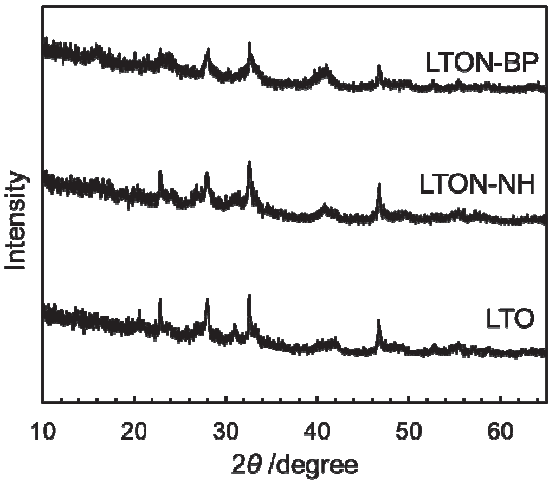

Figure 1 XRD patterns of LTO, LTON-NH, and LTON-BP.

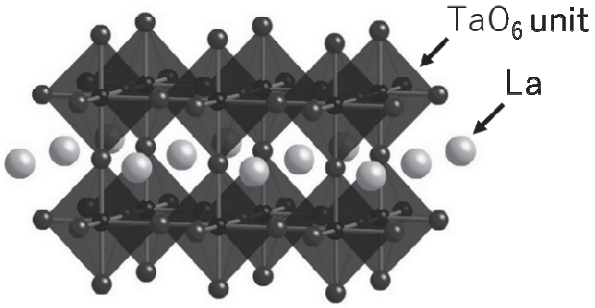

Figure 2 Crystal structure of LTO.

Figure 3 shows SEM images of the prepared samples. Each sample normally exhibits a lateral dimension of the order of microns and a thickness of up to several dozen nanometers. In the case of $LaTa_2O_7$ nanosheets, the thickness of a single layer nanosheet was reported to be approximately of 1.11 nm [13]. Therefore, it can be concluded that the samples used in this study have a plate shape with dozens of stacked layers. The compositions of the samples were

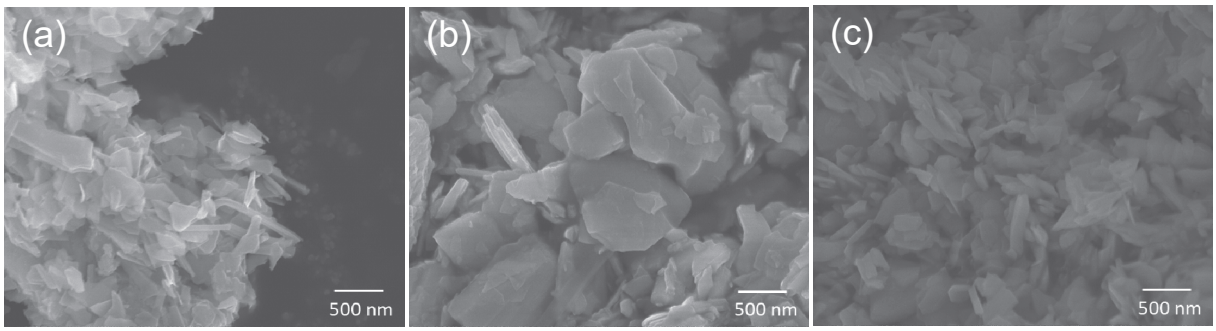

Figure 3 SEM images of (a) LTO, (b) LTON-NH, and (c) LTON-BP.

determined by EDX analysis to be $La_{0.93}Ta_{2.47}O_{6.59}$, $La_{0.92}Ta_{2.62}O_{6.56}N_{0.06}$, and $La_{1.12}Ta_{2.75}O_{6.15}$ for LTO, LTON-NH, and LTON-BP, respectively.

Since nitrogen was not detected in LTON-BP by EDX analysis, an XPS measurement was performed. Figure 4(a) shows the XPS spectra of Ta 4p and N 1s for LTO, LTON-NH, and LTON-BP. The binding energy was normalized by adjusting the C 1s peak to 284.6 eV [14]. In all samples, the Ta 4p peak was observed at 404 eV. Figure 4(b) shows the differential spectra between each LTON nanosheet and LTO. Broad peaks were observed at 397 eV for LTON-NH and at 402 eV for LTON-BP. It was previously reported that nitrogen atoms were doped into the oxygen sites of the metal oxynitride obtained by heating a metal oxide with NH_3, and N 1s peaks were observed at 395.8 to 397.5 eV [15]. In the present study, the N 1s peak of LTON-BP was observed at higher binding energy than that of LTON-NH. Meanwhile, previous studies on N-doped TiO_2 showed that the N 1s peak of nitrogen added at the interstitial crystal lattice was observed at 400 eV [16]. These results suggest that the small amount of nitrogen atoms in LTON-BP was doped not in the oxygen sites but in the interstitial crystal lattice sites. In addition, the fact that the nitrogen atoms added to LTON-BP were detected only in the XPS measurement indicates that LTON-BP contained a high nitrogen concentration near the surface.

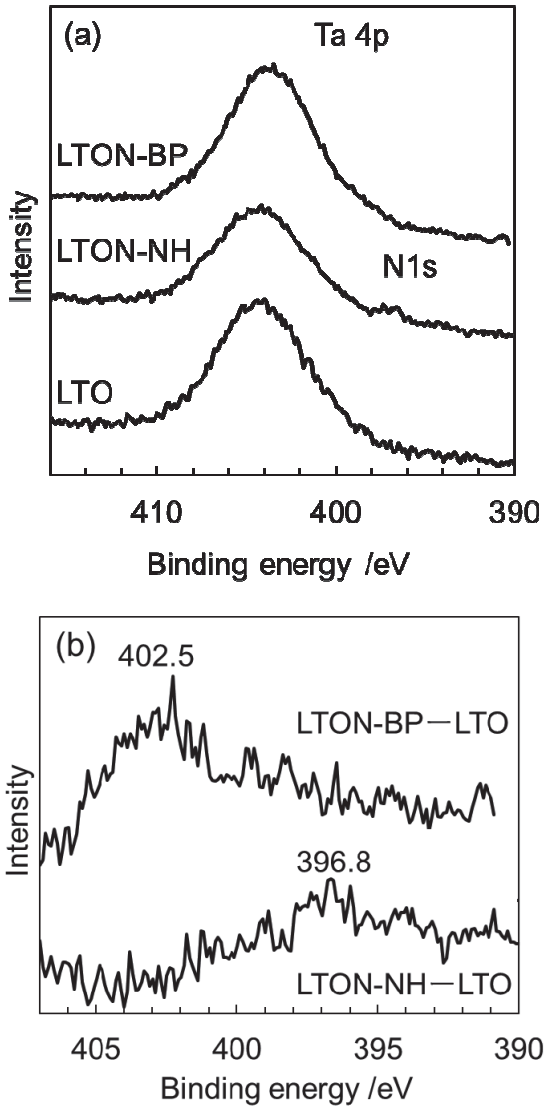

Figure 4 (a) XPS spectra of LTO, LTON-NH, and LTON-BP, (b) Differential XPS spectra between LTON samples and LTO.

Figure 5(a) shows the UV–vis diffuse reflection spectra of the photocatalysts. The absorption edge of LTO, LTON-NH, and LTON-BP were observed at around 300, 600, and 350 nm, respectively. According to previous reports, the valence band maximum of $LaTa_2O_{7-x}N_x$ is more negative than that of $LaTa_2O_7$ because the potential energy of N 2p is

higher than that of O 2p [10]. Therefore, the shift of valence band maximum between LTON-NH and LTON-BP suggests that their photoabsorption properties changed by doping nitrogen. Figure 5(b) shows the Tauc plot of each sample. The band gaps of LTO, LTON-NH, and LTON-BP were estimated to be 3.99, 1.95, and 2.96 eV, respectively, being the narrowing of the band gap of both LTON samples attributable to the effect of the doped nitrogen.

Figure 6 depicts the time course of H_2 production on LTON-BP and LTON-NH from triethanolamine aqueous solution. Both catalysts showed an induction period at the beginning of the reaction, followed by a linear H_2 production phase. The induction period most likely involves the reduction of $Pt(NH_3)_4(NO_3)_2$ and loading of the resulting Pt particles on the photocatalyst. Oxygen formation was not observed on both catalysts, since triethanolamine works as a sacrificial reagent. Under this condition, the photocatalytic reaction can be assumed to proceed as follows [17]:

$$\text{Photocatalyst} + h\upsilon \rightarrow e^-_{(CB)} + h^+_{(VB)} \quad (2)$$

$$2H^+ + 2e^-_{(CB)} \rightarrow H_2 \quad (3)$$

$$N(CH_2CH_2OH)_3 + H_2O + 2h^+_{(VB)} \rightarrow HN(CH_2CH_2OH)_2 + HOCH_2CHO + 2H^+ \quad (4)$$

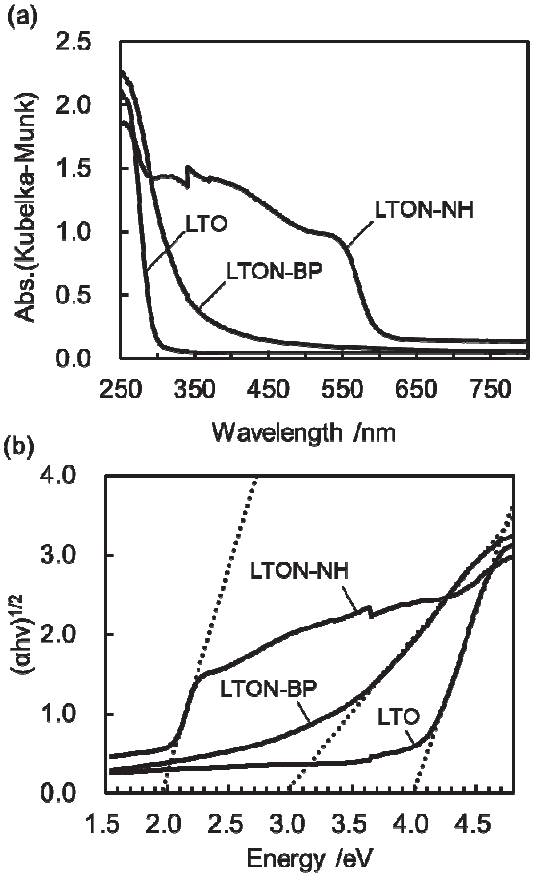

Figure 5 (a) UV–vis diffuse reflectance spectra and (b) Tauc plots of LTO, LTON-NH, and LTON-BP.

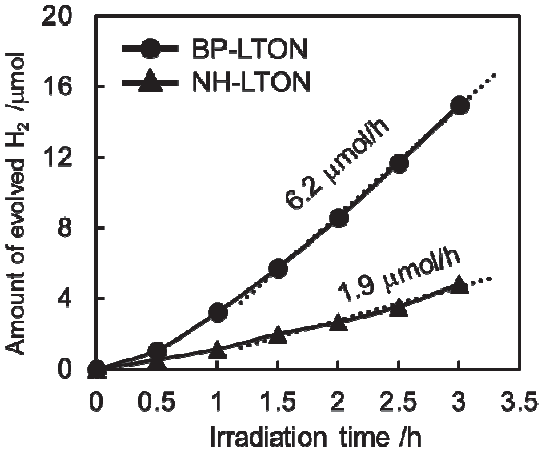

Figure 6 Time course of H_2 formation from 0.75 M triethanolamine aqueous solution under Xe lamp irradiation by Pt/LTON-NH and Pt/LTON-BP.

The formation of H_2 occurred with the concomitant oxidation of triethanolamine. The H_2 production rates were 6.2 mol/h and 1.9 mol/h for LTON-BP and LTON-NH, respectively,

indicating that the activity of LTON-BP was about 3.3 times higher than that of LTON-NH. The difference in the oxidizing power of the photogenerated holes can be invoked to explain the higher activity of LTON-BP. As described above, the valence band maximum of LTON-BP was more positive than that of LTON-NH, being the higher oxidation ability of the photogenerated holes in LTON-BP more suitable for the oxidation reaction of triethanolamine. Other possible reasons for the higher activity of LTON-BP are the difference in charge separation lifetime due to the different surface states of both catalysts and the difference in the loading state of the Pt cocatalyst. These possibilities will be explored in future studies. At this stage, the higher photocatalytic activity of LTON-BP is attributed to the high oxidation ability that stems from its band structure. Although this study only addresses the absorption of UV light by LTON-BP, the light absorption of LTON-BP catalysts can be adjusted by changing the N_2 plasma treatment conditions. Therefore, highly active visible light-responsive photocatalysts can be expected to be developed by optimizing the plasma treatment conditions.

4. Summary

N-doped $LaTa_2O_7$ nanosheets (LTON-BP) were prepared by N_2 plasma treatment, and their photocatalytic activity was compared with that of N-doped $LaTa_2O_7$ nanosheets (LTON-NH) prepared by conventional NH_3 heat treatment and exfoliation. XPS measurements suggest that nitrogen atoms were added at the interstitial crystal lattice sites of LTON-BP. The difference in the band structure of LTON-BP and LTON-NH were also supported by UV–vis diffuse reflectance spectroscopy measurement. Comparison of the photocatalytic activities of LTON-BP and LTON-NH in the H_2 production reaction from aqueous triethanolamine showed that LTON-BP was 3.3 times more active than LTON-NH. This is most likely due to the high oxidation ability of LTON-BP arising from its band structure. The development of highly active visible light-responsive photocatalysts by optimizing N_2 plasma treatment conditions will be the subject of further studies.

Acknowledgment

This research was partially supported by JSPS KAKENHI Grant-in-Aid for Specially Promoted Research (JP16H06293), and a Grant-in-Aid for Scientific Research (C) (JP18K05292).

References

[1] M. Jansen, H. P. Letschert, *Nature*, 404 (2000) 980.

[2] R. Asahi, T. Morikawa, T. Ohwaki, K. Aoki, Y. Taga, *Science*, 293 (2001) 269.

[3] K. Maeda, K. Teramura, D. Lu, T. Takata, N. Saito, Y. Inoue, K. Domen, *Nature*, 440 (2006) 295.

[4] K. Maeda, D. Lu, K. Domen, *Chem. Eur. J.*, 19 (2013) 4986.

[5] S. Balaz, H. S. Porter, M. P. Woodward, J. L. Brillson, *Chem. Mater.*, 25 (2013) 3337.

[6] B. Siritanaratkul, K. Maeda, T. Hisatomi, K. Domen, *ChemSusChem*, 4 (2011) 74.

[7] C. Pan, T. Takata, M. Nakabayashi, T. Matsumoto, N. Shibata, Y. Ikuhara, K. Domen, *Angew. Chem. Int. Ed.*, 54 (2015) 2955.

[8] K. Maeda, K. Domen, *Bull. Chem. Soc. Jpn.*, 89 (2016) 627.

[9] S. Ida, Y. Okamoto, M. Matsuka, H. Hagiwara, T. Ishihara, *J. Am. Chem. Soc.,* 134 (2012) 15773.

[10] M. Lv, X. Sun, S. Wei, C. Shen, Y. Mi, X. Xu, *ACS Nano*, 11 (2017) 11441.

[11] K. Matsubara, M. Danno, M. Inoue, Y. Honda, T. Abe, *Chem. Eng. J.*, 181–182 (2012) 754.

[12] J. Tauc, R. Grigorovici, A. Vancu, *Phys. Status Solidi B*, 15 (1996) 627.

[13] W.-J. Lee, H. J. Yeo, D.-Y. Kim, S.-M. Paek, Y.-I. Kim, *Bull. Korean Chem. Soc.*, 34 (2013) 2041.

[14] P. Swift, *Surf. Interface Anal.*, 4 (1982) 47.

[15] H. Irie, Y. Watanabe, K. Hashimoto, *J. Phys. Chem. B*, 107 (2003) 5483.

[16] F. Peng, L. Cai, H. Yu, H. Wang, J. Yang, *J. Solid State Chem.*, 181 (2008) 130.

[17] D. Bryce-Smith, J. D. Coyle, *SPR Photochemistry*, 11 (1981) 615.